



A molecular phylogeny of Asian barbets: Speciation and extinction in the tropics

Robert-Jan den Tex^a, Jennifer A. Leonard^{a,b,*}

^a Department of Evolutionary Biology, Uppsala University, Norbyvägen 18D, 75236 Uppsala, Sweden

^b Conservation and Evolutionary Genetics Group, Estación Biológica de Doñana (EBD-CSIC), Avd. Américo Vespucio s/n, 41092 Seville, Spain

ARTICLE INFO

Article history:

Received 19 September 2012

Revised 1 March 2013

Accepted 6 March 2013

Available online 16 March 2013

Keywords:

Megalaimidae

LTT plot

Molecular clock

cytb

FIB7

ND2

ABSTRACT

We reconstruct the phylogeny of all recognized species of the tropical forest associated Asian barbets based on mitochondrial and nuclear sequence data and test for the monophyly of species and genera. Tropical regions are well known for their extraordinarily high levels of biodiversity, but we still have a poor understanding of how this richness was generated and maintained through evolutionary time. Multiple theoretical frameworks have been developed to explain this diversity, including the Pleistocene pump hypothesis and the museum hypothesis. We use our phylogeny of the Asian barbets to test these hypotheses. Our data do not find an increase in speciation in the Pleistocene as predicted by the Pleistocene pump hypothesis. We do find evidence of extinctions, which apparently contradicts the museum hypothesis. However, the extinctions are only in a part of the phylogeny that is distributed mainly across Sundaland (the Malay peninsula and the islands off southeast Asia). The theory of island biogeography predicts a higher rate of extinction on islands than on mainland areas. The data from the part of the phylogeny primarily distributed on the mainland best fit a pure birth model of speciation, and thus supports the museum hypothesis.

© 2013 Elsevier Inc. All rights reserved.

1. Introduction

Tropical regions contain a disproportionate amount of biodiversity (Myers et al., 2000), and are also under particular threat due to extraction of resources for export and increasing local human populations (Cincotta et al., 2000; Davies et al., 2006; Woodruff, 2010). The Asian barbets (Aves: Megalaimidae) are a bird family closely related to woodpeckers and the African and South American barbets (Moyle, 2004; Hackett et al., 2008), and may be representative of many tropical forest taxa for several reasons. They are non-migratory, forest dependent, non-passerine birds with relatively poor dispersal (Short and Horne, 2001; Horne and Short, 2002). Only one species, the widespread coppersmith barbet (*Megalaima haemacephala*), expanded across Huxley's line and reached the Philippines (Dickinson et al., 1991) (Fig. 1). Barbets and the closely related toucans inhabit tropical Africa, Asia and America, but the species in each of these three regions have been shown to form monophyletic clades (Moyle, 2004).

The clade of current Asian barbets originated around 31 million years ago (MYA) (Moore and Miglia, 2009) and contains around 30 species (Short and Horne, 2001; Collar, 2006; Feinstein et al., 2008) that are mostly territorial in their breeding behavior (Short and

Horne, 2001). Some of the species are widespread and contain morphologically distinct subspecies. In the last few years, some subspecies have been raised to species based in part on molecular data (Rasmussen and Anderton, 2005; Collar, 2006; Feinstein et al., 2008), and it is possible that more data will identify more divergent units that should be raised to species level.

Three general processes govern the level of biodiversity or species richness in any area: speciation, extinction and dispersal (Wiens and Donoghue, 2004). How the extraordinary level of tropical diversity originated is still debated. Two basic hypotheses are the 'museum hypothesis' and the 'Pleistocene pump' hypothesis. The museum hypothesis explains the high level of biodiversity through low levels of extinction (Mittelbach et al., 2007). The Pleistocene pump hypothesis explains the diversity by high levels of speciation during the Pleistocene as populations diverged and speciated in allopatry and then expanded into sympatry repeatedly as the climate fluctuated.

The Pleistocene pump hypothesis was not formulated specifically for tropical Southeast (SE) Asia (Haffer, 1969), but it seems particularly appropriate for this region (Sodhi et al., 2004; Woodruff, 2010). Unlike the other major tropical regions, SE Asia contains both large areas of mainland and many islands of varying size including Borneo and Sumatra. These islands are on a shallow continental shelf called the Sunda shelf, and were connected with each other and the mainland of SE Asia by large expanses of dry land periodically through the end of the Pliocene and the Pleistocene (Heaney, 1986, 1991; Hall, 1998; Sathiamurthy and Voris, 2006). This cyclical pattern may generate diversity through a pump

* Corresponding author at: Conservation and Evolutionary Genetics Group, Estación Biológica de Doñana (EBD-CSIC), Avd. Américo Vespucio s/n, 41092 Seville, Spain. Fax: +34 954 621125.

E-mail address: JLeonard@ebd.csic.es (J.A. Leonard).

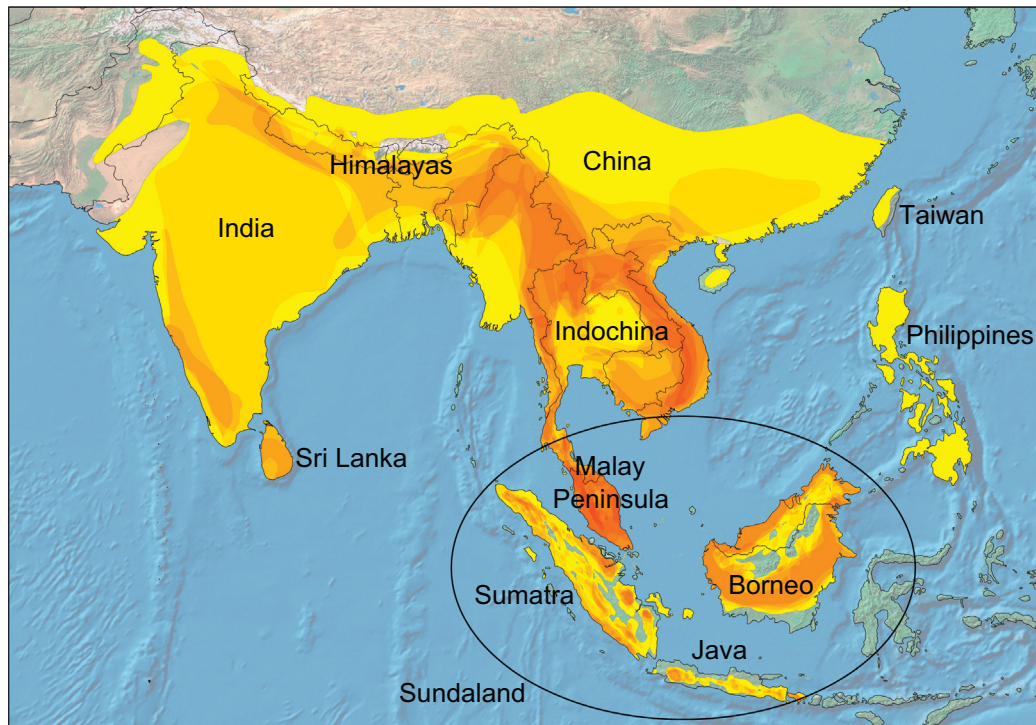


Fig. 1. Map with species distributions of Asian barbets plotted on top of each other. The distribution data are based on Short and Horne (2001, 2002) and for one taxon (*M. faber sini*) on Collar (2006). The more intensely colored the area is, the more species co-occur. White denotes only one species occurs there. The oval approximates encircles the landmasses that comprise Sundaland. The gaps that can be observed on the islands in Sundaland (especially the inland areas of Borneo) and in the Himalayas do not necessarily mean that barbets do not occur there but may reflect a lack of information. (For interpretation of the references to colour in this figure legend, the reader is referred to the web version of this article.)

in which populations of widespread taxa diverge in isolation when sea level is high, and then expand out of their refugia as reproductively isolated species that colonize the other regions when the landmasses are rejoined in times of lower sea levels (Gorog et al., 2004; Lim et al., 2011; Woodruff, 2010). This Pleistocene pump hypothesis predicts an increase in diversification rate starting when the sea level fluctuations start at the end of the Pliocene or as they intensify in the Pleistocene. This can be tested by constructing a phylogeny of all species in the group, and dating the nodes representing speciation.

The museum hypothesis predicts very low levels of extinction, so to reject the museum hypothesis it would be necessary to demonstrate high levels of extinction in tropical taxa. Although the fossil record makes it perfectly clear that the history of life on earth is primarily the history of extinctions (Raup, 1986), actually testing for extinctions using phylogenies is quite difficult (Purvis, 2008; Rabosky, 2010). A serious issue hindering this is that the pattern of temporal diversification yielded by extinctions can also be generated by an increase in diversification rate affecting the whole tree or a rate shift among clades in the phylogenetic tree (Chan and Moore, 2005; Rabosky, 2010). So, in order to demonstrate extinctions it must first be demonstrated that there has not been a change in diversification in the phylogeny. Empirical data from birds most commonly yield a density dependent pattern of speciation (Phillimore and Price, 2008). However, recently developed temporal and topological tree tests now enable changes in rates of cladogenesis along phylogenies to be tested (Rabosky, 2006a; Chan and Moore, 2005). Therefore, if a lineage through time analysis yields a pattern consistent with extinctions, a change in diversification rate can be tested for, and potentially rejected. Topological tree tests can be used to test if there has been a significant rate shift among clades and even identify which branch(es) are affected (Moore et al., 2004; Chan and Moore, 2005) and there-

fore distinguish between a birth death pattern and among clade rate diversification.

Here we construct the complete phylogeny of the Asian barbet species with extensive subspecies sampling, so we are able to test some taxonomic hypotheses within the group. Further, we will use that phylogeny to test two hypotheses that may explain tropical biodiversity. First, the 'Pleistocene Pump' hypothesis that predicts increased diversification at the onset of increased climatic fluctuations (glacial cycles) and associated sea level fluctuations (Lisiecki and Raymo, 2005) around 2.5–3 MYA. Secondly, we test the 'museum' hypothesis, that explains high tropical biodiversity by low rates of extinction in relatively stable environments, by comparing (i) if a rate constant model fits the observed data better than a rate variable model and (ii) which model of rate constant diversification (one with extinction and one without extinction) fits the observed pattern of temporal diversification better.

2. Material and methods

2.1. Materials for DNA sequencing

Twenty-six species of Asian barbets were recognized by Short and Horne (Short and Horne, 2001; Horne and Short, 2002). Since then *Megalaima rubricapilla malabarica* was raised to species level (*M. malabarica*) by Rasmussen and Anderton (2005) and the *M. oorti* group was split into four species (Collar, 2006; Feinstein et al., 2008). This brings the total number of recognized Asian barbet species to 30, all of which are sampled here. Some of these species have large geographic distributions and multiple named subspecies (Berlioz, 1936; Peters, 1948). As many of the subspecies as possible were sampled. When available, at least two individuals of each taxon were included. In total 110 samples were obtained (Table 1). All data collected here is from museum specimens.

Table 1

List of the samples used for this study including their museum numbers, species, subspecies when available, and original collection location. The museum abbreviations are: RMHN AVES for the Netherlands Centre of Biodiversity (NCB) Naturalis, Leiden, The Netherlands; KUNHM for the University of Kansas Museum of Natural History, Lawrence, Kansas; ZMUC for Zoological Museum University of Copenhagen; NRM for the Swedish Museum of Natural History, Stockholm; AMNH for the American Museum of Natural History, New York; LSUMNS for Louisiana State University Museum of Natural Science; and KIZ for Kummung Institute of Zoology, China Academy of Science.

Museum	Catalog no.	Species	Subspecies	Country
RMHN.AVES.	10286	<i>Calorhamphus fuliginosus</i>	<i>hayii</i>	Indonesia
RMHN.AVES.	10287	<i>Calorhamphus fuliginosus</i>	<i>hayii</i>	Indonesia
RMHN.AVES.	162481	<i>Calorhamphus fuliginosus</i>	<i>fuliginosus</i>	Indonesia
RMHN.AVES.	162482	<i>Calorhamphus fuliginosus</i>	<i>fuliginosus</i>	Indonesia
RMHN.AVES.	27053	<i>Megalaima rafflesii</i>	<i>malayensis</i>	Malaysia
RMHN.AVES.	162483	<i>Megalaima rafflesii</i>	<i>rafflesii</i>	Indonesia
RMHN.AVES.	162484	<i>Megalaima rafflesii</i>	<i>rafflesii</i>	Indonesia
RMHN.AVES.	162485	<i>Megalaima rafflesii</i>	<i>rafflesii</i>	Indonesia
RMHN.AVES.	162486	<i>Megalaima rafflesii</i>	<i>rafflesii</i>	Indonesia
RMHN.AVES.	162487	<i>Megalaima rafflesii</i>	<i>billitonis</i>	Indonesia
RMHN.AVES.	162488	<i>Megalaima rafflesii</i>	<i>billitonis</i>	Indonesia
RMHN.AVES.	61626	<i>Megalaima rafflesii</i>	<i>borneensis</i>	Indonesia
RMHN.AVES.	162489	<i>Megalaima rafflesii</i>	<i>borneensis</i>	Indonesia
RMHN.AVES.	162490	<i>Megalaima mystacophanos</i>	<i>mystacophanos</i>	Indonesia
RMHN.AVES.	27050	<i>Megalaima mystacophanos</i>	<i>mystacophanos</i>	Indonesia
RMHN.AVES.	162491	<i>Megalaima mystacophanos</i>	<i>humii</i>	Indonesia
RMHN.AVES.	162492	<i>Megalaima mystacophanos</i>	<i>humii</i>	Indonesia
RMHN.AVES.	162493	<i>Megalaima flavifrons</i>		Sri Lanka
RMHN.AVES.	162494	<i>Megalaima flavifrons</i>		Sri Lanka
RMHN.AVES.	9065	<i>Megalaima franklinii</i>	<i>ramsayi</i>	Thailand
RMHN.AVES.	9064	<i>Megalaima franklinii</i>	<i>ramsayi</i>	Thailand
RMHN.AVES.	81943	<i>Megalaima javensis</i>		Indonesia
RMHN.AVES.	61624	<i>Megalaima javensis</i>		Indonesia
RMHN.AVES.	23437	<i>Megalaima javensis</i>		Indonesia
RMHN.AVES.	162495	<i>Megalaima chrysopogon</i>	<i>chrysopsis</i>	Indonesia
RMHN.AVES.	162496	<i>Megalaima chrysopogon</i>	<i>chrysopsis</i>	Indonesia
RMHN.AVES.	162497	<i>Megalaima chrysopogon</i>	<i>laeta</i>	Malaysia
RMHN.AVES.	162498	<i>Megalaima chrysopogon</i>	<i>laeta</i>	Malaysia
RMHN.AVES.	61614	<i>Megalaima chrysopogon</i>	<i>chrysopogon</i>	Indonesia
RMHN.AVES.	61615	<i>Megalaima chrysopogon</i>	<i>chrysopogon</i>	Indonesia
RMHN.AVES.	10292	<i>Psilopogon pyrolophus</i>		Indonesia
RMHN.AVES.	10294	<i>Psilopogon pyrolophus</i>		Indonesia
RMHN.AVES.	61616	<i>Megalaima corvina</i>		Indonesia
RMHN.AVES.	61617	<i>Megalaima corvina</i>		Indonesia
RMHN.AVES.	162499	<i>Megalaima zeylanica</i>	<i>zeylanica</i>	Sri Lanka
RMHN.AVES.	162500	<i>Megalaima zeylanica</i>	<i>zeylanica</i>	Sri Lanka
RMHN.AVES.	12554	<i>Megalaima lineata</i>	<i>hodgsoni</i>	Thailand
RMHN.AVES.	12555	<i>Megalaima lineata</i>	<i>hodgsoni</i>	Thailand
RMHN.AVES.	23436	<i>Megalaima lineata</i>	<i>lineata</i>	Indonesia
RMHN.AVES.	66807	<i>Megalaima lineata</i>	<i>lineata</i>	Indonesia
RMHN.AVES.	81974	<i>Megalaima lineata</i>	<i>lineata</i>	Indonesia
RMHN.AVES.	10285	<i>Megalaima oorti</i>		Indonesia
RMHN.AVES.	162501	<i>Megalaima oorti</i>		Indonesia
RMHN.AVES.	65804	<i>Megalaima nuchalis</i>		Taiwan
RMHN.AVES.	65803	<i>Megalaima nuchalis</i>		Taiwan
RMHN.AVES.	9069	<i>Megalaima asiatica</i>	<i>davisoni</i>	Laos
RMHN.AVES.	53528	<i>Megalaima asiatica</i>	<i>davisoni</i>	Thailand
RMHN.AVES.	53716	<i>Megalaima asiatica</i>	<i>chersonesus</i>	Thailand
RMHN.AVES.	9063	<i>Megalaima monticola</i>		Malaysia
RMHN.AVES.	162502	<i>Megalaima monticola</i>		Indonesia
RMHN.AVES.	162503	<i>Megalaima monticola</i>		Indonesia
RMHN.AVES.	162504	<i>Megalaima henricii</i>	<i>henricii</i>	Malaysia
RMHN.AVES.	162505	<i>Megalaima henricii</i>	<i>henricii</i>	Indonesia
RMHN.AVES.	162506	<i>Megalaima henricii</i>	<i>henricii</i>	Indonesia
RMHN.AVES.	162507	<i>Megalaima henricii</i>	<i>brachyrhyncha</i>	Indonesia
RMHN.AVES.	162508	<i>Megalaima henricii</i>	<i>brachyrhyncha</i>	Indonesia
RMHN.AVES.	81978	<i>Megalaima armillaris</i>		Indonesia
RMHN.AVES.	82176	<i>Megalaima armillaris</i>		Indonesia
RMHN.AVES.	43427	<i>Megalaima armillaris</i>		Indonesia
RMHN.AVES.	43430	<i>Megalaima armillaris</i>		Indonesia
RMHN.AVES.	40144	<i>Megalaima armillaris</i>	<i>baliensis</i>	Indonesia
RMHN.AVES.	10141	<i>Megalaima armillaris</i>	<i>baliensis</i>	Indonesia
RMHN.AVES.	9133	<i>Megalaima pulcherrima</i>		Malaysia
RMHN.AVES.	9134	<i>Megalaima pulcherrima</i>		Malaysia
RMHN.AVES.	81982	<i>Megalaima australis</i>	<i>australis</i>	Indonesia
RMHN.AVES.	81983	<i>Megalaima australis</i>	<i>australis</i>	Indonesia
RMHN.AVES.	45357	<i>Megalaima australis</i>	<i>australis</i>	Indonesia
RMHN.AVES.	23434	<i>Megalaima australis</i>	<i>australis</i>	Indonesia
RMHN.AVES.	10145	<i>Megalaima australis</i>	<i>hebereri</i>	Indonesia
RMHN.AVES.	10146	<i>Megalaima australis</i>	<i>hebereri</i>	Indonesia
RMHN.AVES.	162509	<i>Megalaima australis</i>	<i>duvaucelii</i>	Malaysia

(continued on next page)

Table 1 (continued)

Museum	Catalog no.	Species	Subspecies	Country
RMHN.AVES.	162510	<i>Megalaima australis</i>	<i>duvaucelii</i>	Malaysia
RMHN.AVES.	61611	<i>Megalaima australis</i>	<i>duvaucelii</i>	Indonesia
RMHN.AVES.	162511	<i>Megalaima australis</i>	<i>duvaucelii</i>	Indonesia
RMHN.AVES.	162512	<i>Megalaima australis</i>	<i>duvaucelii</i>	Indonesia
RMHN.AVES.	162513	<i>Megalaima australis</i>	<i>duvaucelii</i>	Indonesia
RMHN.AVES.	162514	<i>Megalaima eximia</i>		Indonesia
RMHN.AVES.	162752	<i>Megalaima rubricapillus</i>		Sri Lanka
RMHN.AVES.	162751	<i>Megalaima rubricapillus</i>		Sri Lanka
RMHN.AVES.	27059	<i>Megalaima haemacephala</i>	<i>indica</i>	India
RMHN.AVES.	162750	<i>Megalaima haemacephala</i>	<i>indica</i>	Sri Lanka
RMHN.AVES.	162749	<i>Megalaima haemacephala</i>	<i>indica</i>	Sri Lanka
RMHN.AVES.	162745	<i>Megalaima haemacephala</i>	<i>delica</i>	Indonesia
RMHN.AVES.	162746	<i>Megalaima haemacephala</i>	<i>delica</i>	Indonesia
RMHN.AVES.	81987	<i>Megalaima haemacephala</i>	<i>rosea</i>	Indonesia
RMHN.AVES.	66822	<i>Megalaima haemacephala</i>	<i>rosea</i>	Indonesia
RMHN.AVES.	23429	<i>Megalaima haemacephala</i>	<i>rosea</i>	Indonesia
RMHN.AVES.	10151	<i>Megalaima haemacephala</i>	<i>rosea</i>	Indonesia
RMHN.AVES.	10152	<i>Megalaima haemacephala</i>	<i>rosea</i>	Indonesia
RMHN.AVES.	99706	<i>Megalaima haemacephala</i>	<i>celestinoi</i>	Philippines
RMHN.AVES.	99704	<i>Megalaima haemacephala</i>	<i>intermedia</i>	Philippines
RMHN.AVES.	99702	<i>Megalaima haemacephala</i>	<i>intermedia</i>	Philippines
RMHN.AVES.	162748	<i>Megalaima haemacephala</i>	<i>mindanensis</i>	Philippines
RMHN.AVES.	162747	<i>Megalaima haemacephala</i>	<i>haemacephala</i>	Philippines
RMHN.AVES.	97137	<i>Megalaima haemacephala</i>	<i>mindanensis</i>	Philippines
RMHN.AVES.	99703	<i>Megalaima haemacephala</i>	<i>haemacephala</i>	Philippines
KUNHM	10018	<i>Megalaima virens</i>		China
ZMUC	139596	<i>Megalaima viridis</i>		India
NRM	570348	<i>Megalaima faiostricta</i>		Thailand
NRM	570388	<i>Megalaima australis</i>	<i>orientalis</i>	Thailand
KUNHM	10413	<i>Megalaima franklinii</i>	<i>franklinii</i>	China
AMNH	462210	<i>Megalaima malabarica</i>		India
AMNH	777391	<i>Megalaima malabarica</i>		India
AMNH	462209	<i>Megalaima malabarica</i>		India
NRM	570387	<i>Megalaima haemacephala</i>	<i>indica</i>	Thailand
NRM	570386	<i>Megalaima haemacephala</i>	<i>indica</i>	Cambodia
NRM	570385	<i>Megalaima haemacephala</i>	<i>cebuensis</i>	Philippines
NRM	570347	<i>Megalaima lagrandieri</i>		Vietnam
NRM	20086328	<i>Megalaima incognita</i>		Thailand
AMNH	179916	<i>Megalaima asiatica</i>	<i>asiatica</i>	Nepal
LSUMNS ^a	B36365	<i>Calorhamphus fuliginosus</i>	<i>tertius</i>	Indonesia
LSUMNS ^a	B363366	<i>Calorhamphus fuliginosus</i>	<i>tertius</i>	Indonesia
KIZ ^b	13833	<i>Megalaima faber</i>	<i>sini</i>	China
AMNH ^{a,b}	PRS2250	<i>Megalaima franklinii</i>	<i>auricularis</i>	Vietnam
AMNH ^b	DOT9601	<i>Megalaima asiatica</i>	<i>davisoni</i>	?
AMNH ^b	DOT5174	<i>Megalaima nuchalis</i>		Taiwan
AMNH ^b	DOT5175	<i>Megalaima nuchalis</i>		Taiwan
AMNH ^b	647068	<i>Megalaima faber</i>	<i>faber</i>	China
AMNH ^b	647074	<i>Megalaima faber</i>	<i>faber</i>	China
AMNH ^b	646985	<i>Megalaima oorti</i>		Indonesia
AMNH ^b	646996	<i>Megalaima oorti</i>		Indonesia
AMNH ^b	417082	<i>Megalaima annamensis</i>		Vietnam
AMNH ^b	647006	<i>Megalaima annamensis</i>		Laos
AMNH ^b	290488	<i>Megalaima asiatica</i>	<i>davisoni</i>	Vietnam
AMNH ^b	DOT5748	<i>Megalaima asiatica</i>	<i>asiatica</i>	Nepal
LSUMNS ^a	B36354	<i>Megalaima mystacophanos</i>		Indonesia
LSUMNS ^a	B16809	<i>Megalaima lineata</i>	?	?
LSUMNS ^a	B36480	<i>Megalaima monticola</i>		Indonesia
AMNH ^b	DOT9642	<i>Megalaima chrysopogon</i>		?

^a From Moyle (2004).

^b From Feinstein et al. (2008).

Appropriate data from the literature was also included (Moyle, 2004; Feinstein et al., 2008).

2.2. Molecular methods

Extraction of total genomic DNA and set-up of the PCR reactions of the museum specimens was performed in a laboratory especially dedicated to work with low quality/quantity DNA samples as in den Tex et al. (2010a). The DNA was extracted from footpads with DNEasy Tissue Kit (Qiagen) following the manufacturers' instructions. Samples were extracted in small batches and negative

controls were included in every batch in order to monitor for possible contamination.

Fragments were amplified in 25 µl reactions that included 1X Gold Buffer (Applied Biosystems, Foster City, CA, USA), 2.5 mM MgCl₂, 0.2 mM each dNTP, 1 µM of each primer, 1.25 U AmpliTaq Gold DNA polymerase (Applied Biosystems) and between 10 and 50 ng of DNA. The PCR program started with an initial denaturation step of 95 °C for 10 min followed by 36 cycles of 95 °C for 30 s, annealing of 50 °C to 60 °C for 30 s and extension of 72 °C for 45 s with a final extension of 72 °C for 10 min. In all cases negative controls were included to identify possible contamination. Internal

primers for amplifying and sequencing of the mitochondrial cytochrome *b* (*cytb*) gene and the nuclear β -fibrinogen intron 7 (*FIB7*) were designed based on SE Asian barbet sequences available on Genbank. Internal NADH dehydrogenase subunit 2 (*ND2*) gene primers were designed based on sequences obtained from higher quality samples. These internal primers were designed to target 120 base pair (bp) to 300 bp overlapping fragments and used for both PCR and sequencing (Appendix A).

The PCR products were checked on a 2% agarose gel stained with ethidium bromide. Successful amplifications were purified in 25 μ l reactions containing 21 μ l PCR product, 16.8 U of Exonuclease I (New England Biolabs, Ipswich, MA, USA) and 1.68 U of shrimp alkaline phosphatase (USB Corporation, Staufen, Germany) incubated at 37 °C for 15 min followed by 80 °C for 15 min. Both strands of each PCR product were sequenced with BigDye (Applied Biosystems) according to manufacturer's recommendations with the same primers as used for amplification. Sequencing reactions were separated and analyzed on an automated ABI 3730xl DNA Analyzer (Applied Biosystems).

In order to control for possible amplification errors caused by DNA damage, each fragment from all historical specimens was amplified in at least two independent reactions and sequenced in both directions. The sequence fragments were checked, edited and concatenated in Sequencher 4.6 (Gene Codes Corporation, Ann Arbor, MI, USA) into one sequence for each gene.

2.3. Phylogenetic reconstruction

Since not all samples produced complete sequences for all three markers, first a neighbor joining (NJ) tree for each marker (*cytb* $n = 127$, *ND2* $n = 102$ and *FIB7* $n = 100$) was constructed using PAUP* v4.0b10 (Swofford, 2002) based on Timura-Nei distances and ignoring the sites for which data were missing for the pairwise distance calculation. This was done to obtain a first indication of the level of intra-specific divergences and to make sure these markers was informative at this scale. Further, it was used to identify possible amplification of nuclear insertions of mtDNA by looking for spurious (basal) placement of taxa in the phylogenetic tree. The aberrant brown barbet (*Calorhamphus fuliginosus*), distributed on the Malay Peninsula, Sumatra and Borneo, was used as the outgroup because Moyle (2004) showed that is the most basal taxon among SE Asian barbets.

For the reconstruction of the species phylogeny, we reduced the data set by exclusion of very similar and identical haplotypes and the samples with too much missing data. We performed maximum parsimony (MP), maximum likelihood (ML) and Bayesian analysis on this data set ($n = 45$) that consisted of the complete *cytb* (1143 bp), the 5' end of the *ND2* gene (517 bp) and the complete *FIB7* (aligned 627 bp) for most taxa (Table 1). The data were treated as unordered and gaps as missing data. A partition homogeneity test, as implemented in PAUP* v4.10b, was performed to test for incongruence in phylogenetic signal among the three markers. Although *cytb* and *ND2* are both mitochondrial genes and thus linked, these functional genes likely evolve under different constraints, so each gene was tested separately. The ML analysis was performed separately on each gene and the most appropriate model of sequence evolution for each gene was selected based on the AIC score as implemented in Modeltest v3.7 (Posada and Crandall, 1998). The ML analyses used a heuristic search algorithm with tree bisection reconnection (TBR) and 10 random additions per replicate. The MP analysis, using the concatenated dataset, used a heuristic search algorithm with TBR branch swapping and 1000 stepwise random addition replicates. MP support for each node was assessed by 1000 bootstrap replicates using a heuristic search, TBR branch swapping and 10 random additions per replicate.

A Bayesian analysis was performed on the same data set as the MP analysis with MrBayes v3.1.2 (Ronquist and Huelsenbeck, 2003). A three gene-partitioned analysis was conducted that ran for 2 million generations with sampling every 100 generations. A separate analysis used a data partition into four categories namely the nuclear marker and the three codon positions of the two protein coding markers. This analysis ran also for 2 million generations with sampling every 100 generations. Each partition was set its own likelihood model based on model selection results performed with Modeltest v3.7. A 50% majority-rule consensus tree was created for each analysis using a conservative burnin of 25% to calculate Bayesian Posterior Probabilities (PP) to assess nodal support.

A separate Bayesian analysis was performed on the clade that comprised the taxa *M. oorti*, *M. annamenis*, *M. asiatica*, *M. faber*, *M. nuchalis* and *M. incognita* with *M. corvina*, *M. chrysopogon* and *M. monticola* as outgroups. This was based on the *cytb* data only in order to increase taxon sampling and include previously published sequences from individuals from which we did not have samples (Table 1). First, the most appropriate model of sequence evolution per codon position was estimated with Modeltest v3.7 via PAUP* v4.10b. A codon partitioned Bayesian analysis was performed with MrBayes and ran for 2 million generations sampling every 100 generations and used a 25% burnin to obtain the 50% majority-rule consensus tree and calculate Bayesian PP as nodal support. Also a MP analysis and MP bootstrap analysis were conducted using PAUP* v4.10b to obtain support values for the different nodes. The MP analysis used a heuristic search algorithm, TBR branch swapping in which starting trees were obtained by 1000 stepwise random addition replicates. The 1000 replicate bootstrap analysis was performed with a heuristic search, TBR and 10 stepwise random additions per replicate.

2.4. Dating

The molecular dating was based on the two mtDNA genes. There are no internal calibration points available for the Asian barbets so we used age estimates based on mtDNA sequence data on toucans and barbets from South America (Panaté et al., 2009). For the root of all barbet species and the split between the African and South American barbets age estimates based on nuclear sequence data were taken from Moore and Miglia (2009). These two estimates based on different sequence data and calibration points were highly congruent, with the age estimate of the basal South American split of toucans and barbets of 13.4 MYA from Moore and Miglia (2009) and 13 MYA \pm 2.75 MY from Panaté et al. (2009). For use as outgroups, sequences of two species of African barbets and three members of the South American barbet/toucan clade were obtained from Genbank (Africa: *Pogoniulus pusillus* *ND2*: EU166971, *cytb* EU167002.1; *Trachyphonus usambiro* *ND2*: EU166967, *cytb*: EU166982.1; South America: *Pteroglossus inscriptus* *ND2*: AY959854.1, *cytb*: AY959827.1; *Ramphastos toco* *ND2*: GQ458005.1, *cytb*: GQ457988.1; *Semnornis ramphastinus* *ND2*: GQ458015.1, *cytb*: GQ458001.1). In total 51 taxa were included in the dating analyses.

The African and South American taxa were set to be reciprocally monophyletic to each other (Moyle, 2004) and the prior of this split was set to 24.6 \pm 5.9 MYA (Moore and Miglia, 2009) with a normal distribution. The prior of the split between *Pteroglossus* and *Ramphastos* (South American toucans) was set with a normal distribution at 10.75 \pm 2.25 MYA (Panaté et al., 2009) and the South American split between toucans and barbets was set at 13 \pm 2.75 MYA (Panaté et al., 2009). The age of the root was set with a prior normally distributed around 31.5 \pm 9 MYA (Moore and Miglia, 2009).

To obtain Bayesian estimates of the timing of diversification events the program BEAST v1.6.1 (Drummond and Rambaut, 2007) was used with a relaxed clock model with a lognormal distribution and a birth death prior with default parameters. The models of sequence evolution that were identified based on their AIC scores with Modeltest v3.7 were unlinked for the two genes. The prior for the mutation rate of *cytb* was set with a normal distribution around $2.1 \pm 0.68\%$ per MY corresponding with the general finding of Weir and Schluter (2008). The prior for the *ND2* gene was set higher ($3 \pm 1\%$ per MY) based on the estimate on toucans obtained by Panat e et al. (2009). The program ran for 10 million generations with sampling taking place every 1000 generations. A burnin of 25% was applied to obtain the node age estimates and their respective 95% highest posterior density (HPD). The program Tracer v1.5 (Drummond and Rambaut, 2008) was used to assess stationarity of the MCMC chain, parameter effective sample sizes (ESS) and posterior intervals spanning the 95% HPD.

2.5. Test for increase in speciation due to climatic fluctuations

Using the node age estimates from the Beast analysis a lineage through time (LTT) plot was constructed in Excel with the outgroups pruned from the ultrametric tree. We then tested for a significant change in diversification rate during the time period of 2–3.5 MYA with the R package Laser v2.3 (Rabosky, 2006b). This time frame corresponds with the significant increase in climatic oscillations that occurred during the end of the Pliocene and Pleistocene causing periodic land connections between the land masses of the Sunda shelf (Heaney, 1991; Lisiecki and Rambo, 2005). We used the yuleWindow function to obtain model parameters for 4 rate variable models at fixed time points (2, 2.5, 3 and 3.5 MYA) and the pure birth (pureBirth) function and birth death (bd) function for estimates of the rate constant models. The difference between AIC scores of the best rate constant model and the rate variable model was used as test statistic. A negative value for this difference would favor the rate constant model over the rate variable model and a positive value would favor the rate variable model. In our case with 51 taxa, based on the simulations of Rabosky (2006a) a difference in AIC scores of 5 or higher can be used to reject the rate constant model over the rate variable model at $\alpha = 0.05$. We also inferred which model gave the best fit to our temporal data with the function fitdAICrc. The difference in AIC scores can be used to infer if the more complex rate variable model should be favored over the simple rate constant model (Rabosky, 2006a).

To test which rate constant model fit the data best a Likelihood ratio test (LRT) was performed. The rate constant and rate variable models were compared to each other based on differences in AIC scores, and the model with the lowest AIC score was favored. We also used the likelihood ratio test (LRT) to distinguish between the two rate constant models, pure birth and birth death.

2.6. Topological tree tests

We performed a whole tree topology test as implemented in the program SymmeTREE v1.1 (Chan and Moore, 2005). This topological tree test can identify if a significant diversification rate shift among branches has occurred and therefore it can differentiate if the temporal pattern is caused by birth death or a significant shift in diversification rate among clades (Chan and Moore, 2005; Rabosky, 2010). We used the whole tree statistic $M\pi^*$ to test for a diversification rate shift because this statistic shows the highest power to detect such a shift given our 51 taxa tree (Moore et al., 2004). This statistic is based on the comparison of the observed topological distribution of taxon diversity to the expected

distribution of taxa diversity under a equal-rates Markov (ERM) model with the probability of a branching event that is constant for each tip in a growing tree at any instant in time, which we refer to as a pure birth model (Chan and Moore, 2005). To identify which branch(es) are affected by this rate shift, a likelihood score of generating a tree with N taxa partitioned between the left and right descendents of a single node (with l and r taxa, respectively) using a homogeneous rate model was compared to the likelihood score using a rate heterogeneous model. The shift statistics Δ_1 and Δ_2 were used to test for a significant rate shift at a particular node (Moore et al., 2004). We ran SymmeTREE with default settings with the tree topology as generated with the Beast run. Because our phylogeny is well resolved with high support, phylogenetic uncertainty is small.

2.7. Test for extinctions

When a shift in diversification rate along a branch is identified, the tree can be split into subtrees that can be re-analyzed in a temporal framework to test which models would give the best fit to the respective groups with the fitdAICrc function in LASERv2.3. If one of the groups is still identified to be most compatible with a birth death model after branches with increased rates of cladogenesis have been removed, it is most likely that this pattern is not caused by diversification rate shifts among clades but that true extinction has been an important process in shaping the temporal pattern of cladogenesis in that group.

3. Results

3.1. Sequence data and alignment

From the 110 samples (Table 1) only two did not produce any PCR fragment. From the remaining 108, we obtained complete *cytb* (1143 bp) sequences for 93 samples. The complete *ND2* fragment (517 bp) was obtained from 88 individuals. The *FIB7* (627 bp alignment, with slight length variation between taxa due to small indels) was completely sequenced in 70 individuals. No indels were observed in the alignment of the two protein coding genes and they could be translated into amino acid sequences without internal stop codons. Fragments of nuclear origin (NUMTS) can be inadvertently amplified even from historic material (den Tex et al., 2010b) and such copies were identified for the *ND2* gene in *M. oorti*, *M. asiatica chersonesus* and *M. armillaris* and for *cytb* in *M. hamacephala cebuensis*. All NUMTS were excluded from the dataset.

3.2. Phylogenetic reconstructions

The NJ analyses based on the mtDNA genes did not show any spurious phylogenetic placing of intraspecific samples from which we had little sequence data. The ML analysis for each gene yielded one tree in each case and those trees were highly congruent (*cytb* score = 17852.04; *ND2* score = 17340.7; *FIB7* score = 18120.75). The models of sequence evolution used for each gene are given in Table 2.

The partition homogeneity test among the three genes indicated that there was no significant conflict in the underlying phylogenetic signal ($P = 1$). Therefore in both the MP and Bayesian analyses the sequence data were concatenated into one data set.

The MP analysis recovered one tree (tree score = 3333; in total 2287 characters of which 112 were variable but parsimonious uninformative and 756 parsimonious informative characters). MP bootstrap values are high and structure is congruent with the Bayesian tree topology (Fig. 2).

Table 2

A list of the different models of sequence evolution selected for different data partitions based on AIC scores and used for the phylogenetic reconstructions with maximum likelihood and Bayesian methods.

Dataset	Marker	AIC model	Applied model
Complete (n = 42)	<i>cytb</i>	TIM + G + I	GTR + G + I
Complete (n = 37)	<i>ND2</i>	HKY + G + I	HKY + G + I
Complete (n = 38)	<i>FIB7</i>	HKY + G	HKY + G
Complete codon partition (1)	<i>cytb</i> + <i>ND2</i>	GTR + I + G	GTR + I + G
Complete codon partition (2)	<i>cytb</i> + <i>ND2</i>	GTR + I + G	GTR + I + G
Complete codon partition (3)	<i>cytb</i> + <i>ND2</i>	GTR + I + G	GTR + I + G
Dating (n = 51)	<i>cytb</i>	k81uf + G + I	GTR + G + I
Dating (n = 45)	<i>ND2</i>	HKY + G + I	HKY + G + I
Oorti codon partition (1; n = 20)	<i>cytb</i>	TIM + I	GTR + I
Oorti codon partition (2; n = 20)	<i>cytb</i>	TrN	GTR
Oorti codon partition (3; n = 20)	<i>cytb</i>	GTR + G	GTR + G

The Bayesian analysis of the gene partitioned data set yields a well-resolved tree with overall very high Bayesian node supports (>0.95; Fig. 2). No problems were encountered regarding the convergence of the run resulting in good mixing (average split frequency < 0.01) and high parameter ESS values (>200). The results of the four-partitioned data set (three codon positions and the nuclear marker) showed no obvious differences in branch support and topology as compared to the gene partitioned analysis. All informative indels of the nuclear marker are plotted on the Bayesian tree (Fig. 2) and are in complete agreement with the mitochondrial tree topology.

3.3. Species relationships

In most cases the individuals of a given species were monophyletic, but the group of species including and closely related to *M. oorti* is a notable exception. In order to address this clade in more

detail, a phylogeny based only on *cytb* was constructed. This allowed more individuals and localities to be included for these taxa. The MP analysis resulted in 24 MP trees based on 1143 characters of which 77 were variable but parsimonious uninformative characters and 192 parsimony informative characters and with a tree score = 436. The Bayesian analysis recovered a tree topology with most nodes resolved with high support and there is no apparent conflict between the phylogenies constructed with the two different methods of data analysis. Both the Bayesian and MP analysis identified three well-supported clades, but their relationships to each other are still unresolved (Fig. 3).

Some well supported and unexpected relationships are revealed in the phylogeny. First, the species *M. asiatica* was polyphyletic (Fig. 3). A taxon that is only known from a very small area on the Malay Peninsula (Fig. 4), *M. asiatica chersonesus*, is sister to *M. oorti*, and the rest of *M. asiatica* is more closely related to *M. annamensis* (Fig. 2 and 3). This relationship had not been previously hypothesized due to the divergent morphologies of *M. asiatica chersonesus* and *M. oorti*. Second, a highly divergent sequence from *M. asiatica davisoni* from western Thailand is more closely related to *M. annamensis* from Vietnam and Laos than to any other *M. asiatica* in our study. It is unlikely that this sequence constitutes a NUMT because its *ND2* sequence is also strongly divergent from *M. asiatica davisoni* from Laos (the only other *ND2* sequence that is available in this clade). It is most likely that this sequence represents evolution in this lineage as opposed to introgression, because it is also divergent from the next most closely related species, *M. annamensis*. This could suggest the occurrence of a cryptic species. However, further data is required to determine this with certainty.

The close relationship between *M. corvina*, *M. chrysopogon* and *M. monticola* was also unexpected (Fig. 2). Goodwin (1964), however, did suggest a possible close relationship between *M. corvina* and *M. chrysopogon*. The third member of this clade, *M. monticola*, a submontane endemic from Borneo, has formerly been considered

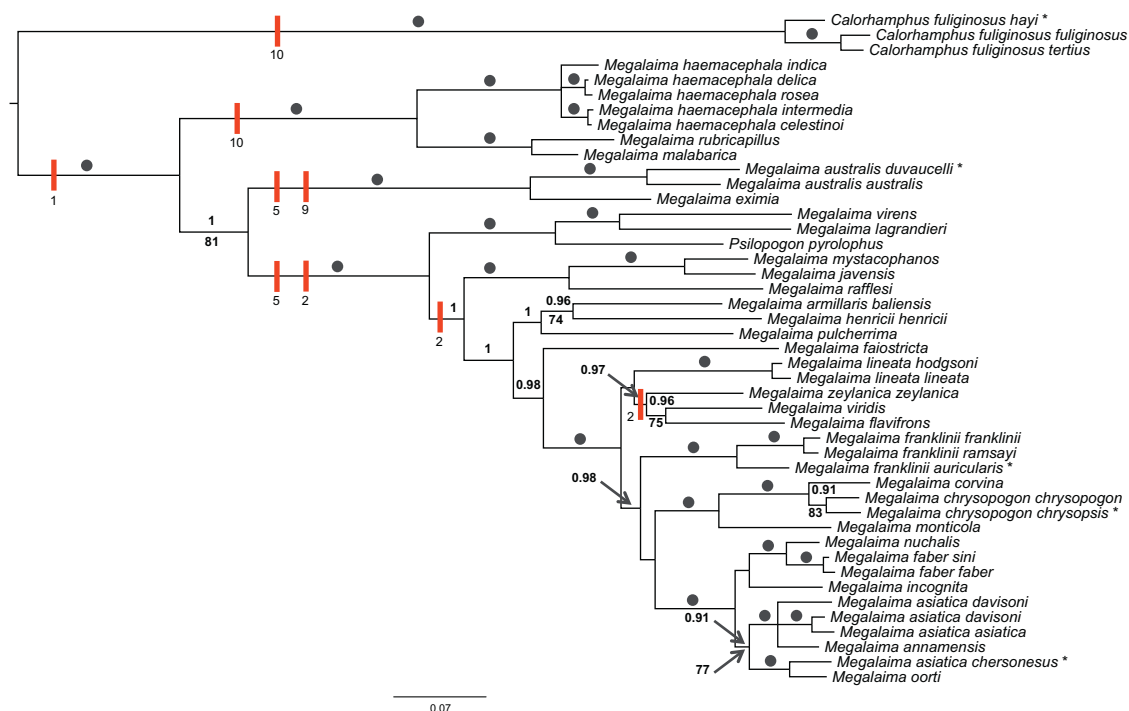


Fig. 2. Bayesian phylogeny of the Asian barbets based on the concatenated dataset (complete *cytb*, partial *ND2* and the complete *FIB7* intron). The dark dots above branches indicate support values of Bayesian posterior probability (PP) = 1 and MP bootstrap ≥ 99 . In other cases the PP value is marked above the branch and the MP bootstrap value below the branch. Unmarked branches have a PP lower than 0.95 or MP bootstrap support lower than 70. The vertical bars drawn on several branches show informative indels in *FIB7* and their length in bp is indicated below. A change in taxonomic status is proposed for the five taxa that are marked with an asterisk.

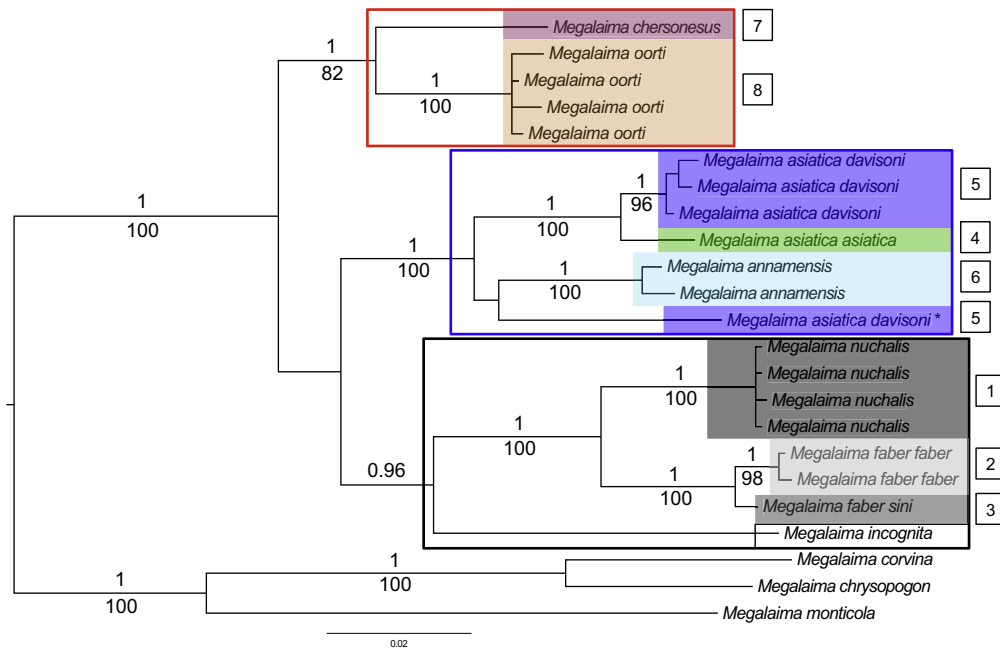


Fig. 3. Bayesian phylogeny based on the *cytb* data (1143 bp) of the *asiatica-oorti-incognita* clade. Above the branches the posterior probability ($PP \geq 0.95$) and below the MP bootstrap values (≥ 70) are indicated. The geographical distribution of the clades boxed with red, blue and black are outlined with the same color in Fig. 4. The numbers to the right of the taxa refer to the numbers in the distribution map (Fig. 4). The Thailand haplotype of *M. asiatica davisoni* is highlighted with an asterisk.

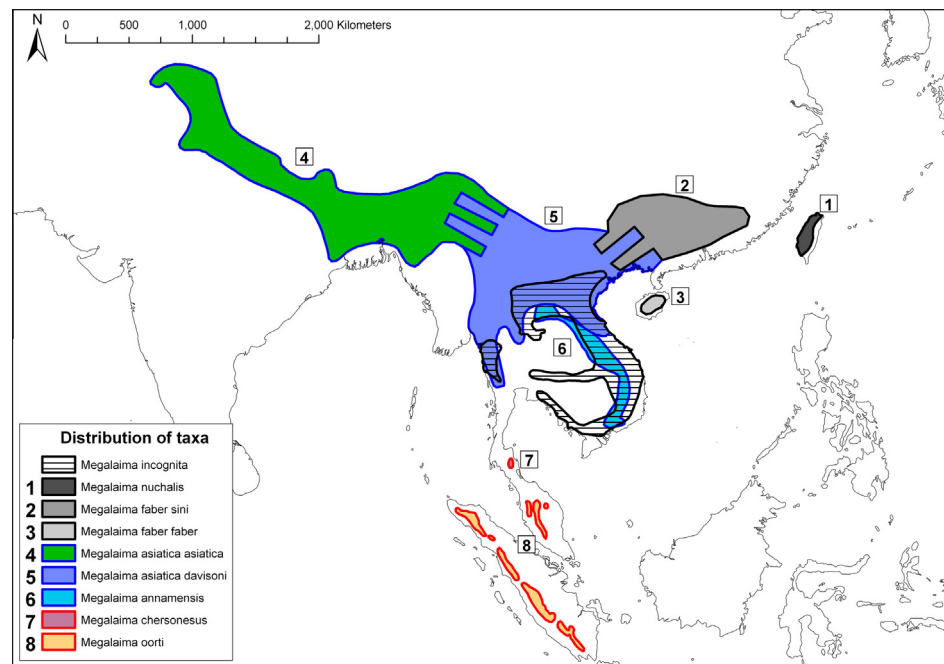


Fig. 4. Distribution map of the taxa comprising the *asiatica-oorti-incognita* clade. The boxed numbers refer to the taxa in the legend and Fig. 3. For taxa 4 and 5 (*Megalaima asiatica asiatica* and *M. asiatica davisoni*) and for taxa 2 and 5 (*M. faber sini* and *M. asiatica davisoni*) the exact amount of overlap is unknown (indicated by the fork-like structure).

a subspecies of *M. oorti* (Chasen, 1935), a subspecies of *M. asiatica* (Peters, 1948) or a monotypic species (Berlioz, 1936; Ripley, 1945; Goodwin, 1964; Short and Horne, 2001; Horne and Short, 2002). Our data clearly supports species status for *M. monticola* (Fig. 5).

Some of the relationships we describe are in closer agreement with previously hypothesized relationships. For example, based on plumage traits *M. faiostricta* was thought to be quite

divergent from all other taxa (Berlioz, 1936) and this is supported by our phylogeny (Fig. 2). The three species *M. henricii*, *M. armillaris* and *M. pulcherrima* have been grouped based on morphology, and we also recover this clade. The proposed split of *M. rubricapilla* by Rasmussen and Anderton (2005) based on morphology and song characteristics is also in agreement with our genetic data.

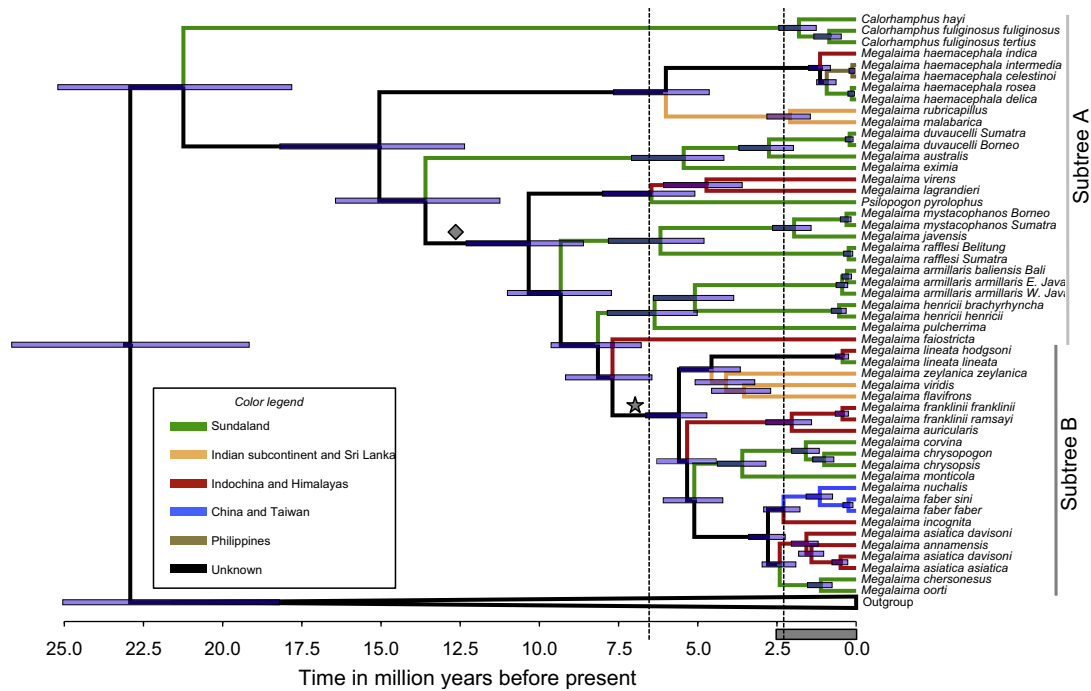


Fig. 5. Dated molecular phylogeny based on the complete mtDNA data set (*cytb* and partial *ND2*). The numbers on the horizontal axis denote time in million of years ago and the grey bar the time interval that corresponds to the Pliocene–Pleistocene climatic fluctuations. The horizontal blue bars illustrate the 95% confidence intervals of the node age estimates. The branches are colored according to where the taxa occur. Sundaland includes of the Malay Peninsula, Sumatra, Borneo, Java and smaller nearby islands. At the bottom of the tree the triangle represents the outgroups used. The star marks the branch along which a near significant change in diversification rate was identified and the splitting of the whole tree into two subtrees A and B is marked with vertical bars on the right. The diamond identifies the branch along which a change in morphology from small sized taxa to medium and large sized taxa. The two vertical dark stippled lines denote the time interval in which the pattern of cladogenesis of the Asian barbets may have experienced an extinction event, see text.

3.4. Divergence time estimation

Based on age estimates obtained from different studies across all birds, Moore and Miglia (2009) derived a molecular clock estimate of 0.456% per MY for the *FIB7* marker in Piciformes and obtained a node age estimate of 31.5 MYA for the start of diversification of extant barbets. The Beast estimate of the root based on mtDNA is 23 MYA (interval 19.32–26.86 MYA). This is very much younger than the date estimated from *FIB7*, the estimate of which is not included in the 95% HPD interval of the mtDNA estimate. Therefore, we explored if older node estimates within the Asian barbets showed incongruence between the *FIB7* age estimate based on ML corrected distances and the mtDNA Beast estimates. The oldest node is the *Calorhamphus* split which Beast estimated to have happened around 21.32 MYA (interval 17.82–25.2 MYA). The *FIB7* estimate is 26.53 MYA, a value that is

not included in the 95% HPD interval of the Beast estimate. The Beast age estimate of the next split, the clade including *Megalaima haemacephala*, is 15.16 MYA (interval 12.36–18.2 MYA), the *FIB7* estimate for this clade is 13.76 MYA. The next clade estimate, the one including *Megalaima australis*, using mtDNA is 13.72 MYA (interval 11.25–16.44 MYA) with the corresponding *FIB7* estimate of 14.17 MYA. These two are more or less in agreement with each other indicating that both markers are able to estimate node ages accurately in this time frame. At shallower time depth (younger than 10–15 MYA) the *FIB7* marker is not reliable for estimating node ages because it is not informative enough. For that reason, most age estimates are younger than those inferred from mtDNA. Taken together, node age estimates based on mtDNA seem to become unreliable at time depths beyond 15–20 MYA, because the models of sequence evolution are unable to properly correct for saturation anymore (Weir and Schluter, 2008). Although the older

Table 3

Summary of the results of the test of the 'Pleistocene pump' hypothesis. Irrespective of the two different age node estimates for *Calorhamphus* (the mtDNA estimate of 21 MYA and the nuclear DNA age estimate of 26 MYA) there is no significant difference between the best rate constant model and the rate variable model over the time interval 3.5–2 MYA.

Time of rate shift	yuleWindowLH1	yuleWindowLH2	AIC score of yuleWindow rate shift model	AIC score best rate constant model	deltaAIC
Inferred change at 3.5 MYA ^a	-7.378425	35.37997	-52.00309	-55.29141	-3.28832
Inferred change at 3.5 MYA ^b	-9.307764	35.37997	-48.144412	-53.07592	-4.931508
Inferred change at 3 MYA ^a	-9.409877	38.42928	-54.038806	-55.29141	-1.252604
Inferred change at 3 MYA ^b	-11.16078	38.42928	-50.537	-53.07592	-2.53892
Inferred change at 2.5 MYA ^a	-8.697611	38.08744	-54.779658	-55.29141	-0.511752
Inferred change at 2.5 MYA ^b	-10.45262	38.08744	-51.26964	-53.07592	-1.80628
Inferred change at 2 MYA ^a	-4.919557	33.83271	-53.826306	-55.29141	-1.465104
Inferred change at 2 MYA ^b	-6.806621	33.83271	-50.052178	-53.07592	-3.023742

^a *Calorhamphus* split at 21 MYA.

^b *Calorhamphus* split at 26 MYA.

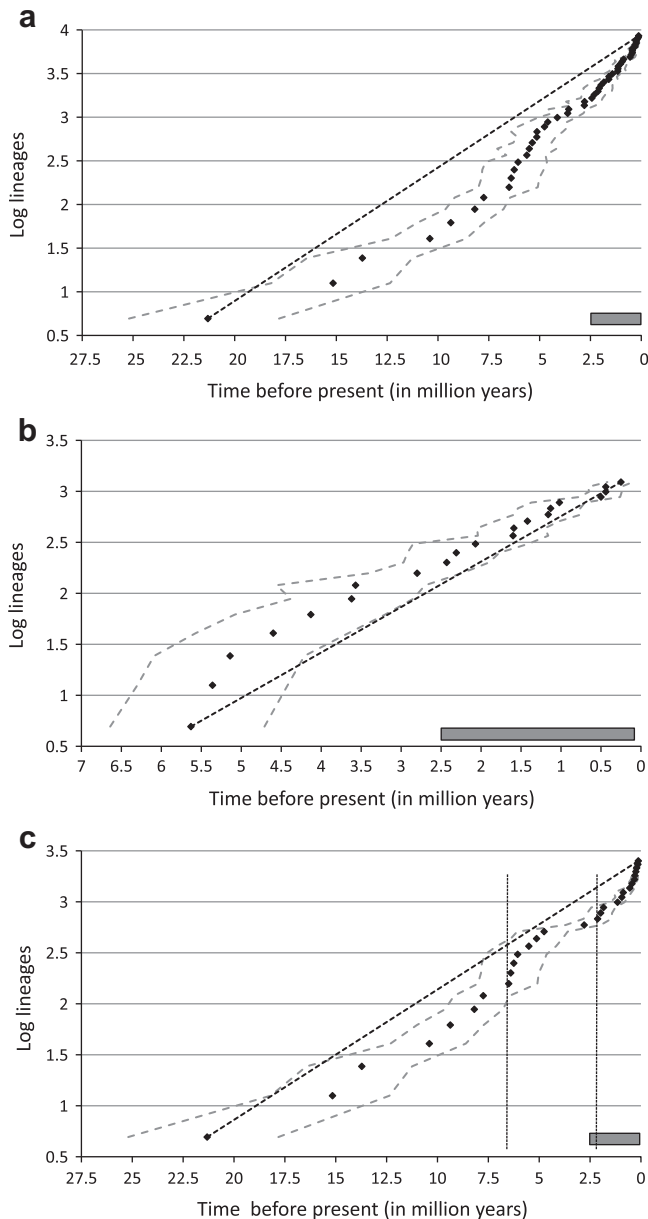


Fig. 6. The lineage through time (LTT) plots of the Asian barbet diversification. On the horizontal axis time in million of years ago is plotted and the vertical axis indicates the natural logarithm of numbers of lineages. The black diamonds are the median node age estimates and the grey stippled lines show the 95% envelope of the highest probability density of the node age estimates. The straight black dotted line illustrates diversification under a constant rate and no extinction (a pure birth model). The grey bar near the time axis illustrates the time interval of increased climatic perturbations starting at the end of the Pliocene. (A) The complete Asian barbet temporal diversification. The best fit model was a birth death model. (B) The LTT plot for subtree B that was identified as evolving under a pure birth model of cladogenesis and (C) the temporal diversification in subtree A that best fit a birth death model of cladogenesis. The two vertical lines indicate a period of possible extinction that is discussed in the text and is also indicated in Fig. 5.

date based on the *FIB7* appears more reliable, all temporal diversification analyses were performed with both node estimates for the *Calorhamphus* split, the Beast estimate from mtDNA of 21.32 MYA and the *FIB7* clock estimate of 26.53 MYA.

The estimates for the molecular rates (parameter meanRate) for the two mitochondrial markers were nearly identical (2.7–3.82 % per MY for *cytb* and 2.68–3.84% for *ND2*). The mean rate for both markers was 3.26% and this is very close to the estimate of Weir

and Schluter (2008) for the Piciformes (3.3%) but is substantially higher estimations than the average rate of 2.1% usually used in birds (Lovette, 2004).

3.5. Diversification through time

No significant rate shift was identified at the onset of the climatic perturbations starting around 3.5 MYA (Table 3). All differences between the AIC score of the best rate constant model (the birth death model, see below) and the rate variable model were negative, irrespective of the age estimate used for the *Calorhamphus* split.

The LTT plot of the complete phylogeny shows a pattern that is most compatible with a birth–death model with a relative high extinction rate (Fig. 6a; Nee, 2006; Rabosky, 2006a; Crisp and Cook, 2009). However, this pattern is also compatible with an overall increase in diversification rate over the whole tree or within certain clades (Rabosky, 2010). The model that best fit the temporal data was a birth death model. There was no significant difference between the best rate constant model and the best rate variable model for the complete barbet phylogeny. Therefore, we cannot reject the rate constant model of diversification for the whole barbet data set. The birth death model was identified as the best fit to the complete dataset irrespective of the two different node age estimates of the *Calorhamphus* split (split at 21 MYA $\chi^2 = 4.39$, $df = 1$, $P = 0.036$; split at 26 MYA $\chi^2 = 6.853$; $df = 1$; $P = 0.009$; Table 4).

3.6. Topological tree test and temporal tests on subtrees

The whole tree statistic $M\pi^*$ showed that the Asian barbet topology differed significantly from a symmetrical tree topology ($P = 0.02$) implying that rate shift(s) in diversification rate have occurred along one or more branches in our tree.

The shift statistics Δ_1 and Δ_2 identified a near significant rate shift along the branch leading to the split between more brownish striped barbets (e.g. *M. lineata* and *M. viridis*) and the group comprising *M. franklinii* and *M. asiatica* ($P(\Delta_1) = 0.05$; $P(\Delta_2) = 0.06$; the branch is marked with a star in Fig. 5). Therefore, the tree was split into two groups. The first group included all taxa that are descendent from the branch that was identified as having undergone a shift in diversification rate (subtree B; $n = 21$). The second group consists of the remaining taxa (subtree A; $n = 29$).

The best fit model for temporal cladogenesis in subtree B was a pure birth model of diversification (Table 4; Fig. 6b). A birth death model was the best fit for subtree A, irrespective of the age estimate for *Calorhamphus* (split at 21 MYA $\chi^2 = 4.219$, $df = 1$, $P = 0.04$; split at 26 MYA $\chi^2 = 6.375$, $df = 1$, $P = 0.012$; Fig. 6c). Estimates of speciation rates λ and extinction rates μ are given in Table 4. Using the two different age estimates of *Calorhamphus* the estimated λ s for subtree A are about the same as the estimated λ for subtree B (Table 4).

4. Discussion

4.1. Taxonomic implications

The taxonomy of the *M. oorti*/black-browed barbet group has recently been identified as problematic (Feinstein et al., 2008). The phylogeny we construct here supports the raising of *M. nuchalis*, *M. annamensis* and *M. faber* to species level, as suggested by Feinstein et al. (2008). Our more complete taxonomic sampling shows that the taxon previously referred to as *M. asiatica chersonesus* is more closely related to *M. oorti* than to any other subspecies of *M. asiatica*. This is highly supported on the phylogeny based on both mitochondrial and nuclear DNA (Figs. 2 and 3), and thus

Table 4

Results of the temporal best model fit analysis to the complete phylogeny of Asian barbets and the two subtrees identified as evolving under different diversification rates by the topological tree test. For the complete data set the best fit is a birth death model. For subtree B the best fit is a pure birth model. The subtree A diversified under a birth death model. The speciation rate is denoted with λ and the extinction rate with μ . The parameters r and a are the diversification rate and the ratio between the extinction rate and the speciation rate respectively.

Model	LH score	$r (= \lambda - \mu)$	AIC	$a (= \mu/\lambda)$	λ	μ	Number of taxa
Pure birth (complete) ^a	27.45065	0.230	-52.90129	0	0.230	0	51
Birth–death (complete) ^a	29.6457	0.115	-55.29141	0.692	0.374	0.258	51
Pure birth (complete) ^b	25.11142	0.219	-48.22284	0	0.219	0	51
Birth–death (complete) ^b	28.53796	0.084	-53.07592	0.789	0.395	0.312	51
Pure birth (subtree A) ^a	-5.874913	0.173	13.74983	0	0.173	0	29
Birth–death (subtree A) ^a	-3.765553	0.059	11.53111	0.826	0.337	0.278	29
Pure birth (subtree A) ^b	-7.6215	0.162	17.243	0	0.162	0	29
Birth–death (subtree A) ^b	-4.434063	0.032	12.86813	0.909	0.358	0.283	29
Pure birth (subtree B) ^a	4.489978	0.352	-6.979957	0	0.352	0	22
Birth–death (subtree B) ^a	4.489978	0.352	-4.979957	0	0.352	0	22
Pure birth (subtree B) ^b	4.489978	0.352	-6.979957	0	0.352	0	22
Birth–death (subtree B) ^b	4.489978	0.352	-4.979957	0	0.352	0	22

^a *Calorhamphus* split at 21 MYA.

^b *Calorhamphus* split at 26 MYA.

supports, together with striking morphological differences between this taxon and its sister *M. oorti*, the raising of this taxon to the species level, *Megalaima chersonesus* (Boden Kloss and Chasen, 1927).

Another well supported surprise was the polyphyly of the subspecies *M. asiatica davisoni*. The three specimens from Vietnam and Laos formed a clade that was sister to the subspecies *M. asiatica asiatica*, which is distributed further to the west in the Himalayas (Fig. 4). The remaining specimen from the southern end of the range of *M. asiatica davisoni* in northern Thailand was very divergent from all of the other *M. asiatica* and was more closely related to *M. annamensis*. Similarly, a divergent lineage of the white-browed piculet (*Sasia ochracea*) was identified in the same region (Fuchs et al., 2008). A more detailed phylogeographic study of these taxa is necessary to clarify the situation.

The taxon originally named *Megalaima franklinii auricularis* by Robinson and Boden Kloss in 1919 is most closely related to the other subspecies of *M. franklinii* as it was originally defined which we were able to include in our study (Table 1). However, the level of divergence between them is deep (Fig. 5) and at least comparable to other divergences observed between well-recognized species such as *M. javensis* and *M. mystacophanos*. Also, they differ markedly in plumage by having a large blue patch on their cheeks and a larger yellow bib that has a black band below it. We therefore suggest to raise this subspecies to species level; *Megalaima auricularis*. We also note that the population of *Megalaima franklinii ramsayi* that is distributed in the high mountains on the Malay Peninsula south of the Isthmus of Kra is morphologically divergent from the other subspecies. We were unable to obtain a sample for analysis, but further research on this taxon could be informative.

The full phylogeny also supports the resurrection of the species *Calorhamphus hayi* (J.E. Gray, 1831), *Megalaima chrysopsis* (Goffin, 1863) and *M. duvaucelli* (Lesson, 1830). Each of these taxa is divergent from its sister taxa in mitochondrial DNA and morphology. Further, *C. hayi* and *M. duvaucelli* are also divergent at the nuclear marker *FIB7*. This brings the current number of barbet species in Asia to 35. It is possible that further species will be identified through finer-scale sampling of more subspecies and populations.

4.2. Key innovation

In the middle of the Miocene, around 13 million years ago, a major morphological shift occurred in a lineage of barbets that probably lived in Sundaland- they got bigger (indicated in Fig. 5 with a diamond). Other forest dependent non-passerine birds in tropical Asia were making this same leap at about the same time,

such as the woodpeckers (Fuchs et al., 2007) and the trogons (Hosner et al., 2010).

This shift in some ways fulfils the criteria of a key innovation. This change in size was possibly in response to competition (in response to expanding passerine birds; Mayr, 2006), and it enabled the lineage to expand into a new adaptive zone. Despite the apparent fulfilment of the criteria for a key innovation, it did not apparently change the diversification rate of the lineage and so this can only be considered an interesting pattern.

4.3. Speciation and extinction

Multiple hypotheses have been proposed to account for the huge amount of biodiversity found in the tropics (Mittelbach et al., 2007). One of the hypotheses is the Pleistocene pump hypothesis (Heaney, 1986; Gorog et al., 2004). This hypothesis suggests that the climatic fluctuations in the last few million years have lead to repeated cycles of populations becoming isolated, diverging, and then expanding. This hypothesis predicts an increase in diversification rates as the climate begins to undergo these climatic fluctuations (glacial cycles). The current distribution should be considered the refugial state (Cannon et al., 2009). We do not find a significant diversification rate change around this time interval (Table 3). So, our data do not support the Pleistocene pump hypothesis. This corresponds well with a lack of genetic structure found across the region within several species of birds (Lim et al., 2011).

Another hypothesis that has been put forth to explain the high number of species in the tropics is the museum hypothesis (Mittelbach et al., 2007). In this case there is more tropical diversity not because of faster speciation, but rather slower extinction rates. This hypothesis predicts that the pattern of speciation in tropical groups should best fit the birth only model of diversification. However, the best fit model of speciation for the phylogeny of tropical Asian barbets is the birth death model (Table 4). This pattern is consistent with both a history of some species diverging and others going extinct and a pattern of speciation without extinction but a change in rate of diversification in a part of the phylogeny. To more accurately characterize the evolutionary history of the lineage, we tested for a change in rate of diversification in the tree, and found one (indicated with a star in Fig. 5). Once this lineage (subtree B in Fig. 5) was removed from the analysis, however, the best fit model of evolution for the remaining taxa (subtree A) still was a birth death model, which strongly suggests that extinction has impacted this group. In further support of extinction in this phylogeny, a step/ gap pattern in the LTT plot (between the dashed lines in

Table A1Table of primers used to amplify *cytb*, *ND2* and *FIB7* in this study.

Locus	Primer name	Sequence
<i>cytb</i>	L14827 ^a	CAC ACT CCA CAC AGG CCT AAT TAA
<i>cytb</i>	BarbND5	TAC CTA GGA TCT TTC GCC CT
<i>cytb</i>	BarbNDgood	CCT CYA CMT CCY TRC ACA AAG G
<i>cytb</i>	BarbFWD 73 cb	ACC CTC CAA CAT CTC AGC ATG
<i>cytb</i>	BarbFWD 157 cb	GCC ACC CAC TAC ACT GCA GAC AC
<i>cytb</i>	BarbFWD 262 cb	GCC TCA TTC TTC TTC ATC TGC AT
<i>cytb</i>	BarbFWD 373 cb	ATA GCA ACA GCT TTC GTA GG
<i>cytb</i>	BarbFWD 493 cb	GCC TGA GCG GGA TTT TCA GT
<i>cytb</i>	BarbFWD 601 cb	CTC CAC GAA TCA GGC TCA AA
<i>cytb</i>	BarbFWD 715 cb	CCC CTC TCA AGC CTA GCC CTA TT
<i>cytb</i>	BarbFWD 814 cb	GAA TGA TAT TTC CTC TTT GC
<i>cytb</i>	BarbFWD 928 cb	AAA TCA AAA CAA CGC ACA AT
<i>cytb</i>	BarbFWD 1009 cb	ACC TGA GTA GGC AGC CAA CC
<i>cytb</i>	BarbREV 161 cb	GTG GCT AGG AGT AAT CCT GT
<i>cytb</i>	BarbREV 239 cb	AT TAG TCA GCC ATA TTG GAC
<i>cytb</i>	BarbREV 320 cb	GA TCC GTA GTA GAA GCC TCG TCC
<i>cytb</i>	BarbREV 422 cb	AA TGA TAT TTG TCC TCA TGG
<i>cytb</i>	BarbREV 551 cb	AA GTG TAA GGC GAA GAA TCG
<i>cytb</i>	BarbREV 659 cb	GAT TTT ATC GCA GTT TGA TG
<i>cytb</i>	BarbREV 776 cb	GG GGT GAA GTT TTC TGG GTC
<i>cytb</i>	BarbREV 833 cb	GC AAA TAG GAA TTA TCA TTC
<i>cytb</i>	BarbREV 983 cb	GT TCA GAA TAG TAT TTG GGA
<i>cytb</i>	BarbREV 1073 cb	GT GAT GGA TGC TAG TTG GCC
<i>cytb</i>	H4a short ^b	AGT CTT TGG TTT ACA AGA CC
<i>ND2</i>	L5215 ^c	TAT CGG GCC CAT ACC CCG AAA AT
<i>ND2</i>	barbNDfwd58	GCA ATC TCA AGY AAC CAY TG
<i>ND2</i>	barbNDfwd202	GCC YTM ATY CTA TTC TCA AG
<i>ND2</i>	barbNDfwd346	CCA GAA GTC CTW CAA GGC TC
<i>ND2</i>	barbNDrev171	CAT YGT RGC TTC RAT KGC TC
<i>ND2</i>	barbNDrev266	AGT TGK GTR ATG TCT CAT TG
<i>ND2</i>	barbNDrev395	GTY GAT AGG AGR AGR GCK GT
<i>ND2</i>	barbNDrev539	GCY AGR ATT TTT CGR GTT TGT G
<i>ND2</i>	H6313 ^d	CTC TTA TTT AAG GCT TTG AAG GC
<i>FIB7</i>	FIB-BI7L ^e	TCC CCA GTA GTA TCT GCC ATT AGG GTT
<i>FIB7</i>	BarbFWD 34 f7	AGA TGA ACT AGA AGC AAA CAG AT
<i>FIB7</i>	BarbFWD 79 f7	CCT GTA CTG ACA TTT TCA AA
<i>FIB7</i>	BarbFWD 128 f7	TCT TTC TGC ATA AGA CTG GGT G
<i>FIB7</i>	BarbFWD 161 f7	TGC TAT ACA GTG CTA TTG GGA G
<i>FIB7</i>	BarbFWD 207 f7	GAG ATA TAT TGT TAA ATT ATG TAC TTT AC
<i>FIB7</i>	BarbFWD 250 f7	CIT CTG AGT AGG CAG AAC TTT
<i>FIB7</i>	BarbFWD 281 f7	ATG CGA CAT GCT ATC TGT CTC
<i>FIB7</i>	BarbFWD 326 f7	ACT GGA GCC AGT ACC AAT A
<i>FIB7</i>	BarbFWD 371 f7	CAG CAC TCC CAC CAC CAT TCT
<i>FIB7</i>	BarbFWD 412 f7	TCC AGA TGT GCT GAT TTG TCT
<i>FIB7</i>	BarbFWD 456 f7	TTA TTT GGT TGC AGA GCA GCA CTA
<i>FIB7</i>	BarbFWD 497 f7	CTG CCC TTG TAA CTG CCA GGA GAA
<i>FIB7</i>	BarbFWD 542 f7	AAC TCA CAG CAA TTT AGA GA
<i>FIB7</i>	BarbREV 98 f7	TTT GAA AAT GTC AGT ACA GG
<i>FIB7</i>	BarbREV 149 f7	CAC CCA GTC TTA TGC AGA AAG
<i>FIB7</i>	BarbREV 182 f7	CTC CCA ATA GCA CTG TAT AGC
<i>FIB7</i>	BarbREV 230 f7	GTA CAT AAT TTA ACA ATA TAT CTC TG
<i>FIB7</i>	BarbREV 270 f7	AAA GTT CTG CCT ACT CAG AAG
<i>FIB7</i>	BarbREV 305 f7	TGA GAA AGA GAC AGA TAG CA
<i>FIB7</i>	BarbREV 344 f7	TAT TGG TAC TGG CTC CAG T
<i>FIB7</i>	BarbREV 391 f7	AGA ATG GTG GTG GCA GTG CTG
<i>FIB7</i>	BarbREV 433 f7	GAC AAA TCA GCA CAT CTG GA
<i>FIB7</i>	BarbREV 479 f7	TAG TGC TGC TCT GCA ACC AAA TAA G
<i>FIB7</i>	BarbREV 520 f7	TTC TCC TGG CAG TTA CAA GGC CAG
<i>FIB7</i>	BarbREV 562 f7	TCT CTA AAT TGC TGT GAG TT
<i>FIB7</i>	BarbREV 590 f7	GCT TAA AAT ACA GCT CAG TAT A
<i>FIB7</i>	FIB-BI7U ^e	GGA GAA AAC AGG ACA ATG ACA ATT CAC

^a Helm-Bychowski and Cracraft (1993).^b Modified from Moyle (2004).^c Johnson and Sorenson (1998).^d Hackett (1996).^e Pritchitko and Moore (1997).

Fig. 6C) matches the pattern of an extinction event, based on simulated data (Crisp and Cook, 2009). According to their model, an extinction event affected Asian barbets at the end of the Pliocene. This is apparently not compatible with the museum hypothesis.

Evolution in the lineage that was removed due to a change in rate of diversification (subtree B in Fig. 5) was most compatible with a different pattern. The pattern of diversification in this lineage best fit the birth only model, the model predicted by the museum hypothesis. This suggests that very few lineages in this clade have gone extinct. This lineage very quickly spread around five million years ago and speciated in several geographic regions, including the entire mainland distribution of the genus from India through the Himalayas to China and throughout Indochina. If additional barbet species are identified in the future, this pattern should be strengthened, not diminished.

The part of the phylogeny for which no evidence of extinctions was identified (subtree B in Fig. 5) has a different, more continental, geographic distribution than the rest of the phylogeny (subtree A in Fig. 5), which is primarily distributed in Sundaland. The theory of island biogeography (MacArthur and Wilson, 1967) predicts higher rates of extinctions on islands than on continents. Extinctions in this tropical forest are only identified in the clade primarily distributed on Sundaland, which is comprised of the Malay Peninsula, which is isolated from mainland Southeast Asia by the biogeographic break around the Isthmus of Kra (Hughes et al., 2003), and numerous islands including Sumatra and Borneo. An end Pliocene extinction event would reflect the increased rate of extinction predicted for recently isolated islands after being connected to the mainland (Heaney, 1986) because this is when major climatic fluctuations began to impact southeast Asia.

The estimates of speciation rates (λ) do not differ between the two subtrees (Table 4). This implies that diversification did not differ between the two regions but that the probability of extinction is much higher in Sundaland than on the Asian mainland. This example of extinction in a tropical clade may therefore be the “exception” to the pure birth model which “proves the rule” of the museum hypothesis.

Acknowledgments

This study would have not been possible with the generous help of the following individuals and museums: Jon Fjelså and the Zoological Museum University of Copenhagen (ZMUC, Copenhagen), Paul Sweet and the American Museum of Natural History (AMNH, New York), Ulf Johansson and the Naturhistoriska riksmuseet (NMH, Stockholm), Mark Robbins and the Natural History Museum, the University of Kansas (KUNHM, Kansas) and René Dekker, Hein van Grouw and Steven van der Mije and the Netherlands Centre for Biodiversity Naturalis (NCB) Leiden, The Netherlands. Alberto Castello is thanked for invaluable help with preparing the distribution maps. This project was funded by the Spanish Government (CGL2010-21524), and the Swedish Research Council.

Appendix A.

See Table A1.

References

- Berlioz, J., 1936. Étude critique des capitonidés de la région orientale. *L'oiseau* 6, 28–56.
- Cannon, C.H., Morley, R.J., Bush, A.B.G., 2009. The current refugial rainforests of Sundaland are unrepresentative of their biogeographic past and highly vulnerable to disturbance. *Proc. Nat. Acad. Sci. U.S.A.* 106, 11188–11193.
- Chan, K.M.A., Moore, B.R., 2005. SymmeTREE: whole-tree analysis of differential diversification rates. *Bioinformatics* 21, 1709–1710.
- Chasen, F.N., 1935. A handlist of Malaysian birds. *Bull. Raffl. Mus.* 11, 1–389.
- Cincotta, R.P., Wisniewski, J., Engelman, R., 2000. Human population in the biodiversity hotspots. *Nature* 404, 990–992.
- Collar, N.J., 2006. A taxonomic reappraisal of the Black-browed Barbet *Megalaima oorti*. *Forktail* 22, 170–173.
- Crisp, M.D., Cook, L.G., 2009. Explosive radiation or cryptic mass extinction? Interpreting signatures in molecular phylogenies. *Evolution* 63, 2257–2265.

- Davies, R.G., Orme, C.D.L., Olson, V., Thomas, G.H., Ross, S.G., Ding, T.-S., Rasmussen, P.C., Stattersfield, A.G., Bennett, P.M., Blackburn, T.M., Owens, I.P.F., Gaston, K.J., 2006. Human impacts and the global distribution of extinction risk. *Proc. Roy. Soc. B* 273, 2127–2133.
- Den Tex, R.-J., Thorington, R., Maldonado, J.E., Leonard, J.A., 2010a. Speciation dynamics in the SE Asian tropics: putting a time perspective on the phylogeny and biogeography of Sundaland tree squirrels, *Sundasciurus*. *Mol. Phylogenet. Evol.* 55, 711–720.
- Den Tex, R.-J., Maldonado, J.E., Thorington, R., Leonard, J.A., 2010b. Nuclear copies of mitochondrial genes: another problem for ancient DNA. *Genetica* 138, 979–984.
- Dickinson E.C., Kennedy, R.S., Parkes, K.C., 1991. Birds of the Philippines. An Annotated Checklist. BOU Checklist No. 12. British Ornithologists' Union, Tring, UK.
- Drummond, A.J., Rambaut, A., 2007. BEAST: Bayesian evolutionary analysis by sampling trees. *BMC Evol. Biol.* 7, 214.
- Drummond, A.J., Rambaut, A., 2008. *Tracer version 1.4*. Computer Program and Documentation Distributed by the Author. Available form: <http://beast.bio.ed.ac.uk/Tracer>.
- Feinstein, J., Yang, X., Li, S.-H., 2008. Molecular systematics and historical biogeography of the Black-browed Barbet species complex (*Megalaima oorti*). *IBIS* 150, 40–49.
- Fuchs, J., Ohlson, J.I., Ericson, P.G.P., Pasquet, E., 2007. Synchronous intercontinental splits between assemblages of woodpeckers suggested by molecular data. *Zool. Scr.* 36, 11–25.
- Fuchs, J., Ericson, P.G.P., Pasquet, E., 2008. Mitochondrial phylogeographic structure of the white-browed piculet (*Sasia ochracea*): cryptic genetic differentiation and endemism in Indochina. *J. Biogeogr.* 35, 565–575.
- Goodwin, D., 1964. Some aspects of taxonomy and relationships of barbets (Capitonidae). *IBIS* 106, 198–220.
- Gorog, A.J., Sinaga, M.H., Engstrom, M.D., 2004. Vicariance or dispersal? Historical biogeography of three Sunda shelf murine rodents (*Maxomys surifer*, *Leopoldamys sabanus* and *Maxomys whiteheadi*). *Biol. J. Linn. Soc.* 81, 91–109.
- Hackett, S.J., 1996. Molecular phylogenetics and biogeography of tanagers in the genus *Ramphocelus* (Aves). *Mol. Phylogenet. Evol.* 5, 368–382.
- Hackett, S.J., Kimball, R.T., Reddy, S., Bowie, R.C.K., Braun, E.L., Braun, M.J., Chojnowski, J.L., Cox, W.A., Han, K.-L., Harshman, J., Huddleston, C.J., Marks, B.D., Miglia, K.J., Moore, W.S., Sheldon, F.H., Steadman, D.W., Witt, C.C., Yuri, T., 2008. A phylogenomic study of birds reveals their evolutionary history. *Science* 320, 1763–1768.
- Haffer, J., 1969. Speciation in Amazonian forest birds. *Science* 165, 131–137.
- Hall, R., 1998. The plate tectonics of Cenozoic SE Asia and the distribution of land and sea. In: Hall, R., Holloway, J.D. (Eds.), *Biogeography and Geological Evolution of SE Asia*. Backhuys Publishers, Leiden, the Netherlands, pp. 99–131.
- Heaney, L.R., 1986. Biogeography of mammals in SE Asia: estimates of rates of colonization, extinction and speciation. *Biol. J. Linn. Soc.* 28, 127–165.
- Heaney, L.R., 1991. A synopsis of climatic and vegetational change in Southeast Asia. *Clim. Change* 19, 53–61.
- Helm-Bychowski, K., Cracraft, J., 1993. Recovering phylogenetic signal from DNA sequences: relationships within the corvine assemblage (class aves) as inferred from complete sequences of the mitochondrial DNA cytochrome-b gene. *Mol. Biol. Evol.* 10, 1196–1214.
- Horne, J.F.M., Short, L.L., 2002. Family Capitonidae (Barbets). In: del Hoyo, J., Elliot, A., Sargatal, J. (Eds.), *Handbook of the Birds of the World*, vol. 7. Lynx Edicions, Barcelona, Spain, pp. 140–219.
- Hosner, P.A., Sheldon, F.H., Lim, H.C., Moyle, R.G., 2010. Phylogeny and biogeography of the Asian trogons (Aves: Trogoniformes) inferred from nuclear and mitochondrial DNA sequences. *Mol. Phylogenet. Evol.* 57, 1219–1225.
- Hughes, J.B., Round, P.D., Woodruff, D.S., 2003. The Indochinese-Sundaic faunal transition at the Isthmus of Kra: an analysis of resident forest bird species distributions. *J. Biogr.* 30, 569–580.
- Johnson, K.P., Sorenson, M.D., 1998. Comparing molecular evolution in two mitochondrial protein coding genes (cytochrome b and ND2) in the dabbling ducks (Tribe: Anatini). *Mol. Phylogenet. Evol.* 10, 82–94.
- Lim, C.L., Rahman, M.A., Lim, S.L.H., Moyle, R.G., Sheldon, F.H., 2011. Revisiting Wallace's haunt: coalescent simulations and comparative niche modeling reveal historical mechanisms that promoted avian population divergence in the Malay Archipelago. *Evolution* 65, 321–334.
- Lisiecki, L.E., Raymo, M.E., 2005. A Pliocene-Pleistocene Stack of 57 globally distributed benthic $\Delta 18O$ records. *Paleoceanography* 20, PA1003.
- Lovette, I.J., 2004. Mitochondrial dating and mixed support for the '2% rule' in birds. *Auk* 121, 1–6.
- Mayr, G., 2006. First fossil skull of a Palaeogene representative of the Pici (woodpeckers and allies) and its evolutionary implications. *IBIS* 148, 824–827.
- MacArthur, R.H., Wilson, E.O., 1967. *The theory of island biogeography*. Princeton University Press, Princeton, New Jersey.
- Mittelbach, G.G., Schemske, D.W., Cornell, H.V., Allen, A.P., Brown, J.M., Bush, M.B., Harrison, S.P., Hurlbert, A.H., Knowlton, N., Lessios, H.A., McCain, C.M., McCune, A.R., McDade, L.A., McPeck, M.A., Near, T.J., Price, T.D., Ricklefs, R.E., Roy, K., Sax, D.F., Schluter, D., Sobel, J.M., Turelli, M., 2007. Evolution and the latitudinal diversity gradient: speciation, extinction and biogeography. *Ecol. Lett.* 10, 315–331.
- Moore, W.S., Miglia, K.J., 2009. Woodpeckers, toucans, barbets, and allies. In: Hedges, S.B., Kumar, S. (Eds.), *The Timetree of Life*. Oxford Univ. Press, Oxford, UK, pp. 445–450.
- Moore, B.R., Chan, K.M.A., Donoghue, M.J., 2004. Detecting diversification rate variation in supertrees. In: Bininda-Emonds, O.R.P. (Ed.), *Phylogenetic Supertrees: Combining Information to Reveal the Tree of Life*. Kluwer Academic Publishers, Dordrecht, the Netherlands, pp. 487–533.
- Moyle, R.G., 2004. Phylogenetics of barbets (Aves: Piciformes) based on nuclear and mitochondrial DNA sequence data. *Mol. Phylogenet. Evol.* 30, 187–200.
- Myers, N., Mittermeier, R.A., Mittermeier, C.G., da Fonseca, G.A.B., Kent, J., 2000. Biodiversity hotspots for conservation priorities. *Nature* 403, 853–858.
- Nee, S., 2006. Birth-death models in macroevolution. *Annu. Rev. Ecol. Evol. Syst.* 37, 1–17.
- Panaté, J.S.L., Weckstein, J.D., Aleixo, A., Bates, J.M., 2009. Evolutionary history of *Ramphastos* toucans: molecular phylogenetics, temporal diversification, and biogeography. *Mol. Phylogenet. Evol.* 53, 923–934.
- Peters, J.L., 1948. *Check-List of the Birds of the World*, vol. 6. Harvard University Press, Cambridge (MA), Massachusetts.
- Phillimore, A.B., Price, T.D., 2008. Density-dependent cladogenesis in birds. *PLOS Biol.* 6, 483–489.
- Posada, D., Crandall, K.A., 1998. Modeltest: testing the model of DNA substitution. *Bioinformatics* 14, 817–818.
- Prychitko, T.M., Moore, W.S., 1997. The utility of DNA sequences of an intron from the -Fibrinogen gene in phylogenetic analysis of woodpeckers (Aves: Picidae). *Mol. Phylogenet. Evol.* 8, 193–204.
- Purvis, A., 2008. Phylogenetic approaches to the study of extinction. *Annu. Rev. Ecol. Evol. Syst.* 39, 301–319.
- Rabosky, D.L., 2006a. Likelihood methods for detecting temporal shifts in diversification rates. *Evolution* 60, 1152–1164.
- Rabosky, D.L., 2006b. LASER: a maximum likelihood toolkit for detecting temporal shifts in diversification rates from molecular phylogenies. *Evol. Bioinform. Online* 6, 257–260.
- Rabosky, D.L., 2010. Extinction rates should not be estimated from molecular phylogenies. *Evolution* 64, 1816–1824.
- Rasmussen, P.C., Anderton, J.C., 2005. *Birds of South Asia. The Ripley Guide*, vols. 1 and 2. Smithsonian Institution and Lynx Edicions, Washington, DC, Barcelona.
- Raup, D.M., 1986. Biological extinctions in earth history. *Science* 231, 1528–1533.
- Ripley, S.D., 1945. The barbets. *Auk* 62, 542–563.
- Ronquist, F., Huelsenbeck, J.P., 2003. MrBayes 3: Bayesian phylogenetic inference under mixed models. *Bioinformatics* 19, 1572–1574.
- Sathiamurthy, E., Voris, H.K., 2006. Maps of Holocene sea level transgression and submerged lakes on the Sunda Shelf. *Nat. Hist. J. Chulalongkorn Univ.* 2 (Suppl.), 1–43.
- Short, L.L., Horne, J.F.M., 2001. *Toucans, Barbets and Honeyguides*. Oxford Univ. Press, Oxford, UK.
- Sodhi, N.S., Loh, L.P., Brook, B.W., Ng, P.K.L., 2004. Southeast Asian biodiversity: an impending disaster. *Trends Ecol. Evol.* 19, 654–660.
- Swofford, D.L., 2002. PAUP*4.10b. *Phylogenetic Analysis Using Parsimony (* and Other Methods)*. Sinauer Associates, Sunderland, Massachusetts.
- Weins, J.J., Donoghue, M.J., 2004. Historical biogeography, ecology and species richness. *Trends Ecol. Evol.* 19, 639–644.
- Weir, J.T., Schluter, D., 2008. Calibrating the avian molecular clock. *Mol. Ecol.* 17, 2321–2328.
- Woodruff, D.S., 2010. Biogeography and conservation in Southeast Asia: how 2.7 million years of repeated environmental fluctuations affect today's patterns and the future of the remaining refugial-phase biodiversity. *Biodivers. Conserv.* 19, 919–941.